SANAEE, R., OLUYEMI, G.F., HOSSAIN, M. and OYENEYIN, M.B. 2013. Stress effects on flow partitioning in fractured reservoirs: equivalent porous media versus poro-elasticity coupled modeling. In *Pyrak-Nolte, L.J., Morris, J., Chan, A., Rostami, J. and Dershowitz, W. (eds.) Proceedings of the 47th U.S. rock mechanics/geomechanics American Rock Mechanics Association (ARMA) symposium 2013, 23-26 June 2013, San Francisco, USA*. Alexandira, VA: American Rock Mechanics Association (ARMA), 3, pages 2329-2337.

Stress effects on flow partitioning in fractured reservoirs: equivalent porous media versus poro-elasticity coupled modeling.

SANAEE, R., OLUYEMI, G.F., HOSSAIN, M. and OYENEYIN, M.B.

2013

Stress effects on flow partitioning in fractured reservoirs: equivalent porous media versus poro-elasticity coupled modeling

Sanaee, R.
Robert Gordon University, Aberdeen, United Kingdom
Oluyemi, G.F. and Hossain, M.
Robert Gordon University, Aberdeen, United Kingdom
Oyeneyin, M.B.
Robert Gordon University, Aberdeen, United Kingdom

This paper was prepared for presentation at the 47th US Rock Mechanics / Geomechanics Symposium held in San Francisco, CA, USA, 23-26 June 2013.

ABSTRACT: In this paper the effects of overburden stress on fracture-matrix flow partitioning were numerically analyzed using two different numerical approaches; the analysis was validated using a fractured Clashach core flood laboratory experimental data. In the first numerical approach, the fracture aperture variation under different overburden stresses, measured using a back calculation method based on the treatment of the fracture as an equivalent porous medium, was adopted in a coupled Darcy law, Brinkman flow and Navier-Stokes fluid flow formulation. In the second numerical approach, poro-elasticity was applied in order to accurately account for fracture aperture change under overburden stress loading. The resulting displacements were coupled to the same fluid flow equations used in the first approach through a moving mesh technique. This was further coupled with stress dependent permeability within the matrix. Flow partitioning from the two numerical approaches were compared to the experimental data. This comparison highlighted the inefficiency of treating fractures as equivalent porous medium. Moreover the cross-flow between the fracture and the matrix was monitored in both modeling approaches and a critical stress beyond which the matrix can no longer feed the fracture was identified. This critical stress can be very important in designing production scenarios for highly-stressed fractured reservoirs.

1. INTRODUCTION

Reservoir fluid flow characterization through fractured hydrocarbon bearing formations has always been a major challenge for reservoir engineers. Fracture-matrix flow partitioning is one of a number of factors responsible for this challenge. Flow partitioning is complex, and the complexity increases when the reservoir experiences a varying stress field such as in active tectonic regions or when reservoir depletion causes changes in in-situ stress regime. A comprehensive understanding of the fluid flow partitioning between fracture networks and porous rock matrix demands consideration of stress-related factors. These factors govern the quality of the fracture networks as well as their geometry and flow characteristics. In addition it is important to consider the different fluid flow regimes which occur in the porous medium and within the free flow channels of fracture network.. Stress regime also dictates the permeability of the porous medium through alteration of the pore volume and pore throats.

The first analytical efforts aimed at illustrating the flow behavior within fractured reservoirs are those which consider both fracture and matrix as equivalent identical porous media [1]. This approach can be useful for fractured formations with dense but widely distributed fractures in which the fractures are not the dominant flow paths. However these conditions are not true for most cases of fracture-matrix flow.

As different physics are involved in the flow partitioning phenomenon, numerical modeling seems to be a more promising approach for realistic investigations. So far, a considerable amount of numerical studies which consider fractures as the main flow paths in fractured reservoirs have been carried out. In these numerical studies, finite difference technique was used primarily to model flow within fractures while analytical matrix-fracture transfer models were used to account for matrix contributions [2]. Later on, multi-phase flow [3] within fractures in petroleum reservoirs and more complicated fracture networks in subsurface aquifers were analyzed using finite element discretization and unstructured meshing capabilities [4, 5, 6, 7, 8]. These numerical approaches do not consider any coupled mechanical models and are only applicable to fracture flow studies where stress regime is stable.

Coupled fluid flow models which use a modified parallel plate permeability model for flow in fractures and account for the flow in matrix under stress was introduced in 1994 [9]. These models were examined through finite element simulations for fractured porous media in Cartesian [10] and in radial [11] coordinates. However, these models were based on the assumption that there was no cross flow between the fractures and the matrix which is an over-simplification. Moreover there was no evidence that these models were validated against experimental data.

Very recently flow partitioning was studied within a fractured matrix using a rather different numerical method [12]. In this study laminar single phase Navier-Stokes equations were used for the fracture system whilst Darcy law was used for the porous medium. Although this approach provided a useful fracture flow partitioning (the percentage of the cumulative flow which travels through fractures) model; however, it was based on 2D fracture profiles and did not consider the coupled effects of stresses. Moreover the fracture walls were assumed to be impermeable and so the modeling did not account for cross flow between the matrix and the fracture.

In this paper, a fractured core flooding data obtained under varying overburden stresses was modeled using two different approaches. In the first approach the fracture aperture change was measured by considering the fracture as an equivalent porous medium; whilst in the second approach it was measured by poro-elasticity physics. The other distinguishing factor in the second approach was the use of stress dependent permeability in the matrix in order to obtain the most realistic numerical modeling that perfectly matches available experimental data. However, in both approaches the fracture aperture change was coupled to Navier-Stokes and Darcy equations to describe flow through fractures and the rock matrix respectively. To maintain continuity in the flow between the two systems, Brinkman equation was used.

2. PROBLEM DESCRIPTION

A single-phase oil flooding experiment of a longitudinally fractured core plug [13] was simulated using two different approaches. The problem geometry was constructed by generating cylindrical porous volumes and a rectangular open volume representing core plug and the fracture space respectively. A mapped rectangular gridding pattern was used within the fracture volume to minimize the effects of large aspect ratio difference between the matrix volume and micro-scale fracture. Subsequently the simulated fractured core plug was flooded under various overburden stresses as shown in Fig. 1.

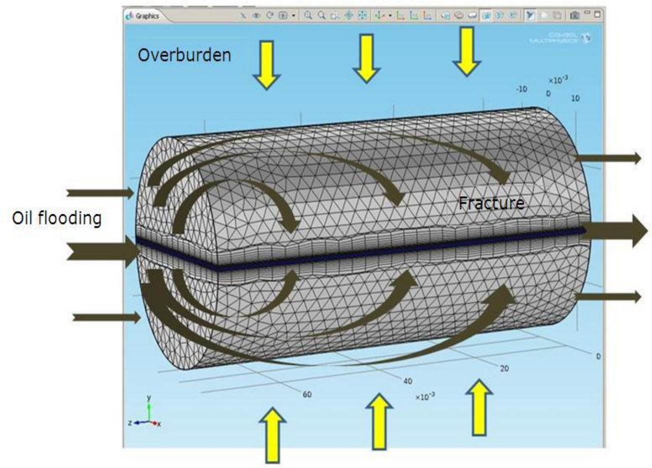

Fig. 1. Model of the simulated fractured core plug.

The experimental differential pressures data was used as boundary conditions and outflow from rock matrix and fracture were monitored within the simulation. Table 1 presents the rock and fluid characteristics which have been used in the simulations. The rock mechanical data for the simulations were typical values for the specific sandstone.

Table 1. Core flooding experimental data

Core diameter	3.79e-2 m
Core length	7.54e-2 m
Matrix porosity	0.154
Matrix permeability	3.10874e-13 m^2
Oil viscosity	0.001 Pa.s
Oil Density	850 kgm^{-3}
Young's Modulus	40e9 Pa
Poisson's ratio	0.14
Compressibility	3e-10 Pa^{-1}

3. MODELING STRESS EFFECTS ON FRACTURE-MATRIX FLOW PARTITIONING: EQUIVALENT POROUS MEDIUM MODELING APPROACH

In this approach, the fracture aperture size under a range of overburden stresses was obtained through a back calculation from flow measurement based on the integration of parallel plate theory and Darcy law [13]. This method was premised on the treatment of the fracture as an equivalent porous medium. Having obtained the aperture size for each overburden stress loading scenario, the geometry was created and fluid flow equations were implemented in the free and porous media flow interface of COMSOL Multi-physics to investigate the fracture-matrix flow partitioning as detailed in the subsections below.

3.1. Governing Equations

Within the rock matrix, Darcy law was applied as the governing equation for flow. This law assumes that the variation of the velocity field when a fluid passes a porous medium is caused by the fluid pressure gradient, viscosity and the trajectory that the fluid travels through as given below in Eq. (1):

$$u = -\frac{k}{\mu}(\nabla P + \rho g \nabla D) \tag{1}$$

In the above equation u is the fluid Darcy velocity, k is the porous medium permeability, μ the fluid dynamic viscosity, ∇P is the pressure gradient, ρ is the fluid density, g is the gravitational acceleration and ∇D is the unit vector in the direction over which the gravity would take effect. In this study, gravity effect has been ignored and therefore the pressure gradient acts as the sole source of oil movement in the core plug. Eq. (1) was combined with the continuity equation in our finite element analysis to provide the generalized governing equation given by Eq. (2):

$$\frac{\partial}{\partial t}(\rho\varphi) + \nabla . P\left[-\frac{k}{\mu}(\nabla P + \rho g \nabla D)\right] = Q_m \tag{2}$$

φ in this equation represents the material porosity and Q_m is a mass source term. Since our simulations were carried out on the basis that the core was fully saturated prior to flooding, a steady state solution with no flow accumulation was considered.

On the other hand, within the fracture, the laminar form of Navier-Stokes equations was used as it was considered a free flow channel; this can be written for an incompressible, constant viscosity fluid as Eq. (3):

$$\nabla P = -\rho\frac{Du}{Dt} + \rho g + \mu\nabla^2 u \tag{3}$$

In order to maintain a continuous velocity and pressure field in the interface of a porous medium and a free flow domain, Brinkman equation which is an extension of Darcy law was adopted. Brinkman equation for a steady-state flow neglecting the inertial forces and any mass generation or accumulation can be written as Eq. (4) [14]:

$$\nabla P = -\frac{\mu}{k}u + \mu_e \nabla^2(u) \tag{4}$$

In this equation μ_e is the effective viscosity of the fluid in the porous medium and free flow domains. μ_e was determined on the assumption that $\mu\frac{du}{dy}$ in free flow domain equals $\mu_e\frac{du}{dy}$ in the porous medium domain when $y = 0$ represents the interface between the domains.

3.2. Flow Partitioning Results

Although the change in the fracture aperture size in this approach was not measured through poro-elastic properties of the core plug, the utilized flow equations provide a continuous flow between the rock matrix and the fracture and allows the cross flow between the two systems. Another important downside of this approach is that for all the overburden stresses, the matrix flow partitioning remains constant since the stress dependent permeability was not accounted for. The flow partitioning results for all the overburden stresses considered are shown in Fig. 2.

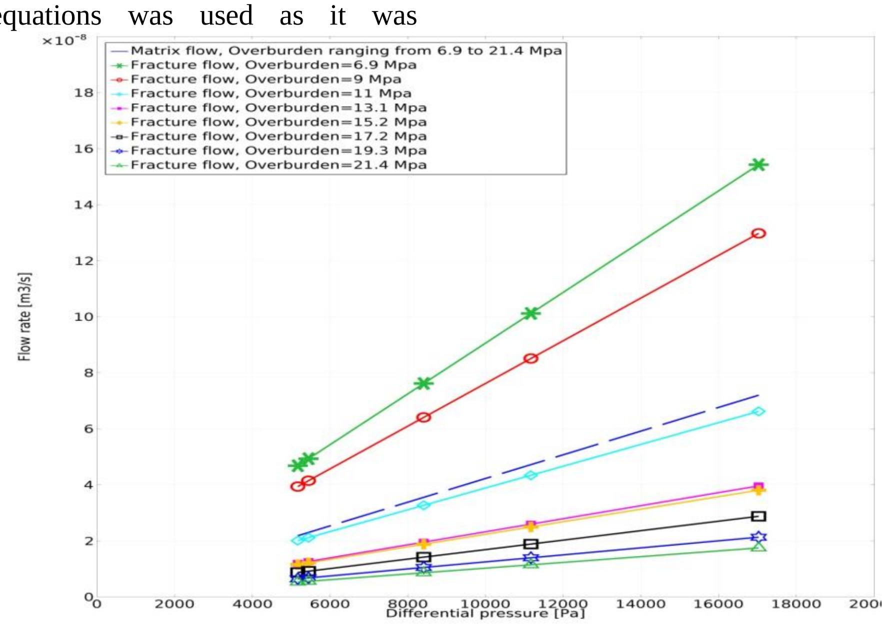

Fig. 2. Fracture and matrix flow rates under various overburden stress loading; this is based on various fracture aperture sizes obtained from equivalent porous medium back calculations of the experimental fracture flow magnitudes.

As expected, fracture flow decreases as the overburden stress increases. Fracture flow results exhibit a rather close trend for fracture flow rates under overburden stress loading above 13e6 Pa while below this stress loading, the flow rate trends are more dispersed; this can be an indication of a shift in stress effects. The dashed marker-free blue line in the figure represents matrix flow; and since stress dependent permeability was not accounted for in this modeling approach, it is unchanged for all the stress loadings. The other inference from the study which is worth noting is that fracture flow exceeds matrix flow at low stress regimes and reduces drastically with increase in overburden stress loading. Consequently a stress threshold is reached beyond which the fracture flow does not change significantly. This is considered as the fracture healing pressure. However poro-elasticity coupled modeling is required to achieve more practical and realistic results.

4. MODELING STRESS EFFECTS ON FRACTURE-MATRIX FLOW PARTITIONING: PORO-ELASTICITY AND STRESS DEPENDENT PERMEABILITY COUPLED ANALYSIS

4.1. Fracture Geometry Change due to poro-elasticity

4.1.1 Governing Equations

In order to obtain the most realistic fracture geometry variation due to overburden stress, poro-elasticity physics was implemented in the finite element analysis. Poro-elasticity combines a transient type of Darcy equation with the elastic stress-strain geomechanical factors. A major constitutive equation in this physics is the Biot's equation (Eq. 5) which relates total stress to the total strain and pore pressure:

$$\sigma = E\varepsilon - \alpha_B P_P \tag{5}$$

In this equation σ is the stress tensor, ε is the strain tensor, E is the elasticity matrix for drained condition, α_B is the Biot-Willis coefficient and P_P is the pore pressure.

Biot's theory [15] delivers the other important constitutive model of poro-elasticity (as given in Eq. 6) which relates the change in the fluid content (ξ) to the volumetric strain (ε_{vol}) and incremental pore pressure:

$$P_P = M(\xi - \alpha_B \varepsilon_{vol}) \tag{6}$$

The coefficients α_B and M have been measured by Biot and Willis [15] as a function of drained, solid and fluid compressibilities. M is the inverse of storage coefficient which appears in Darcy law; this relationship enables the coupling of poro-elasticity equation with Darcy equation in porous medium.

4.1.2 Poro-elasticity Displacements Results

The same laboratory experiment was simulated again using the poro-elasticity fundamentals. 1e6 Pa fracture fluid pressure and pore pressure was defined as the experiment was done at this pore pressure. Boundary conditions were set in a way that the initial fracture aperture was assumed to be about 1.3e-4 m. This assumption is in line with the laboratory requirement to keep the fracture open through the use of shims at the initial stage of flooding.

Having set the initial and boundary conditions, the overburden stress was increased incrementally from 6.9e6 Pa to 2.14e7 Pa and the geometrical displacements were monitored as shown in Fig. 3.

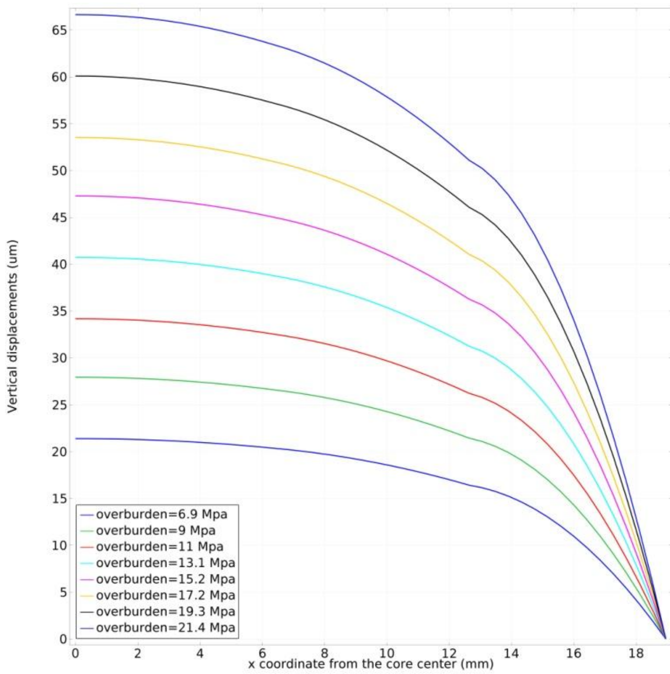

Fig. 3. Vertical displacements of the upper half of the fractured core along the core radius. Note that the origin of the x axis represents the core centre.

As Fig. 3 indicates, the vertical displacements increase as the overburden stresses increases. Displacement is zero at the edge of core where shims are placed initially.

4.2. Poro-elasticity Displacement coupling with Flow Mechanisms

4.2.1 Coupled Governing Equations

The overburden stress has a twofold effect on the fractured porous medium flow. It influences the fracture flow by exerting changes to the fracture aperture and on the other hand it affects matrix flow through alteration of pore throats and the initial permeability of the rock. Both of these effects need to be accommodated in the flow characterization to achieve reliable results.

To consider the changes in the fracture flow, a moving mesh capability was adopted to couple the displacement results to the fracture geometry in the Navier-Stokes flow equations. Moving mesh is an automatic re-meshing that can assist in moving the mesh nodes at each step of the numerical solution when the model geometry is moving, without the need to regenerate the whole meshing process. This scenario was the case for our fractured core under overburden stress loading. The interface between fracture and matrix was allowed to move in prescribed directions and the model automatically perturbed the mesh nodes to conform the moved boundaries. It is worth mentioning that the material properties also extrapolate in the newly generated grids and in this way the material was also moving in accordance with the mesh while the mass balance was kept stable. As the mesh moved at each overburden stress based on the displacements from poro-elasticity calculations, the new conformed mesh was used for the flow calculations.

On the other hand, a stress dependent permeability model (Eq. 7) was used for the matrix flow based on the differential stress and geomechanical properties of the rock for every overburden stress corresponding to the fracture flow calculations [9]:

$$k = k_0\{1 \mp \frac{1}{2}\left[\frac{9(1-\nu^2)}{2}\left(\frac{\pi\Delta\sigma}{E}\right)^2\right]^{\frac{1}{3}}\}^2 \qquad (7)$$

In this equation k_0 represents the initial permeability of the rock matrix, ν is the Poisson's ratio, $\Delta\sigma$ is the differential volume stress and E is the Young's modulus of the drained rock matrix.

In summary, the vertical displacements of the fracture walls (derived from Eq.5 and Eq.6 calculations) were updating the fracture aperture while moving mesh capability was conforming the mesh according to the deformed fracture geometry. The updated fracture was used in the same flow equations used in the equivalent porous medium approach to obtain the fracture flow for each overburden stress. Simultaneously Eq.7 delivered updated matrix flow by changing the matrix permeability according to the overburden stress.

4.2.2 Geomechanically Coupled Flow Partitioning Results

Having coupled the stress dependent permeability for the matrix and updated displacements from poro-elasticity and implemented the meshing of the interactive flow in the fracture and matrix, the simulations were performed for different stress regimes with the aim of investigating the change in the flow between the fracture and the matrix. The results of these simulations are presented in Fig. 4.

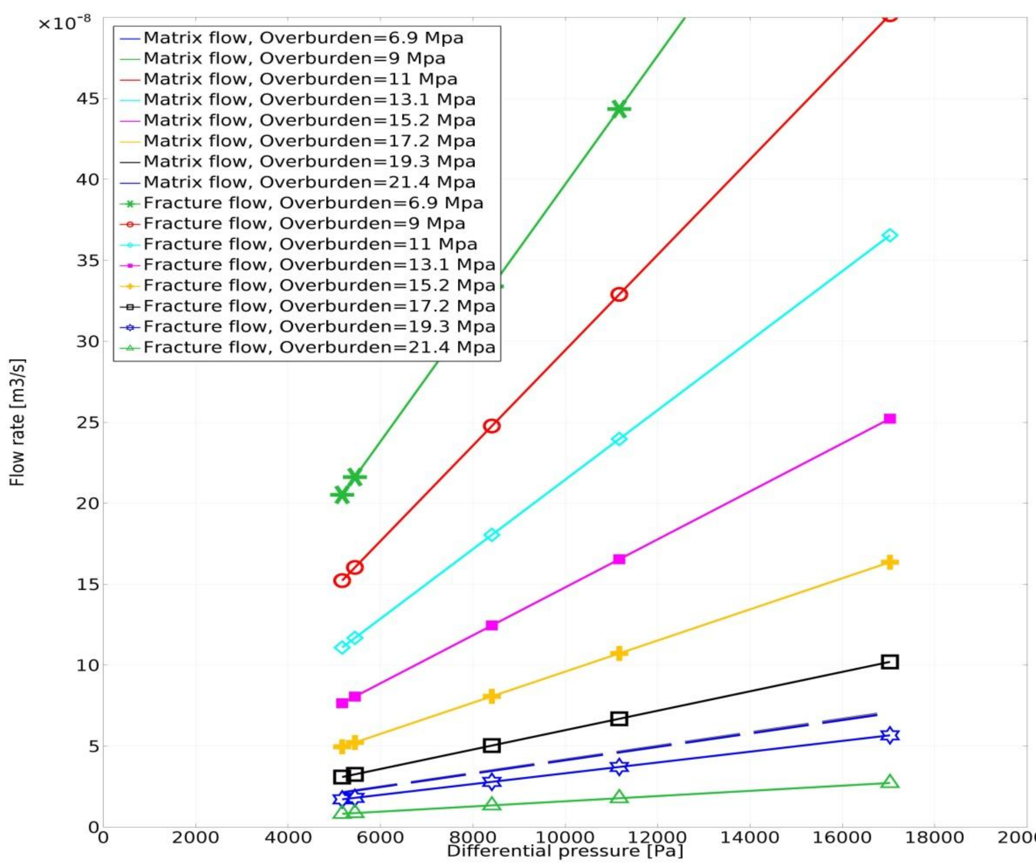

Fig. 4. Matrix and fracture flow rates under various overburden stresses in the coupled poro-elasticity and stress dependent permeability modeling.

Fig. 4 indicates that the coupled analysis provides higher flow rates through the fracture in comparison with the results of the equivalent porous medium approach (Fig. 2) by tens of mm^3/s, while for the matrix the results from the two approaches are rather the same. Furthermore, in contrast to the equivalent porous medium approach, the fracture is the main flow path for most of overburden stress loading. In order to achieve a better understanding of the results, it should be considered that in the poro-elasticity coupled approach the fracture was kept open at a fixed aperture size in the fracture edges and the surface average of the fracture contraction over its plane under stress is being applied as the fracture aperture size change. However, in the equivalent porous medium approach, it was assumed that the fracture aperture was completely affected by the stress regimes and it decreased monotonically throughout the whole fracture plane. This resulted in slightly increased fracture aperture in the poro-elasticity coupled approach.

5. VALIDATION OF RESULTS

The ideal approach to validating the modeling results would be to compare the individual matrix and fracture flow obtained from the modeling with the same experimental flow data. However, because this experimental data was not available, the cumulative outflow results from the two approaches were compared with the experimental flooding data [13]. The equivalent porous medium approach results match the experimental data within 10% error margin whilst, the poro-elasticity and stress dependent permeability coupled approach results exhibit a much closer match of the experimental data to within 5% error margin as shown in Fig. 5 for 2.14e7 Pa overburden stress.

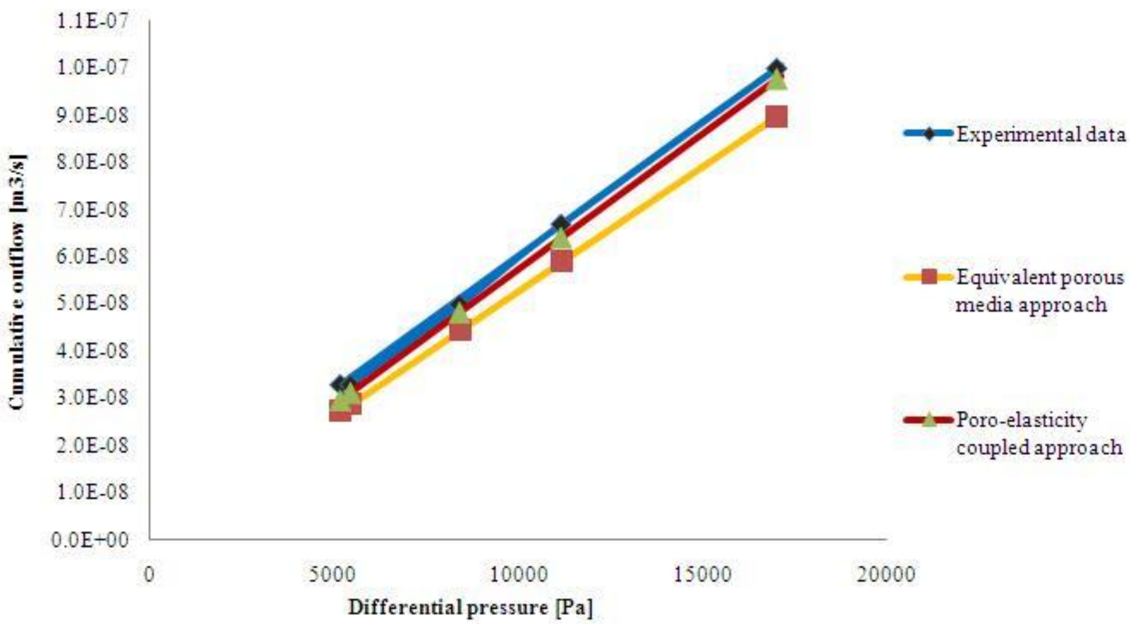

Fig. 5. Comparison of the cumulative outflow results obtained from poro-elasticity and stress dependent permeability coupled approach and equivalent porous media approach with experimental data for 2.14e7 Pa overburden stress. Note the better match of the poro-elasticity coupled modeling approach.

6. DISCUSSION

Although the changes in the flow rates seem to be infinitesimal, attention is drawn to the fact that these are flow rate changes for a small core plug and even a 5 percent change in flow rates here is a considerable flux in field scale investigations. Furthermore, treating fractures as equivalent porous media is quite prevalent when dealing with dense fractured reservoirs, however the comparison provided in this study reveals that this practice can be so misleading.

Matrix flow partitioning results from poro-elasticity coupled modeling approach seem to be identical to the results from equivalent porous media approach (when Fig. 2 is compared with Fig. 4). However it must be noted that this similarity is only as a result of scale effects on fracture flow plots in Fig. 4. To emphasize the change in the matrix flow for the poro-elasticity coupled modeling, the resulting flow rates for the extreme cases of overburden stresses are plotted in Fig. 6. Similarly the change is not so impressive for our small core plug case; however, it can be so significant for large blocks of reservoir rock in highly stressed regions.

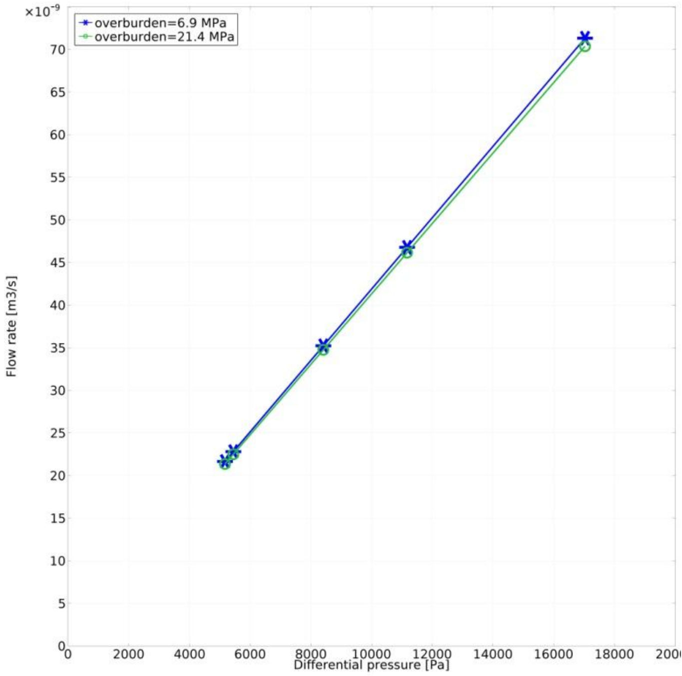

Fig. 6. Matrix flow rate change in response to the overburden stress from the poro-elasticity coupled modeling approach.

The importance of this work lies in its potential application to the alteration of cross flow between the fracture and the matrix in a fractured porous system especially when reservoir engineers count on the large matrix blocks to feed the existing fracture networks in order to maintain reservoir deliverability. Coupling of Brinkman flow equation to the Darcy's law and Navier-Stokes equation at the interface between the fracture and the matrix provides the chance to monitor the cross flow and also follow its variation in a fully geomechanically-coupled simulation. Fig. 7 presents the cross flow magnitudes from the equivalent porous medium modeling whilst Fig. 8 provides their rate and variation from the poro-elasticity coupled modeling.

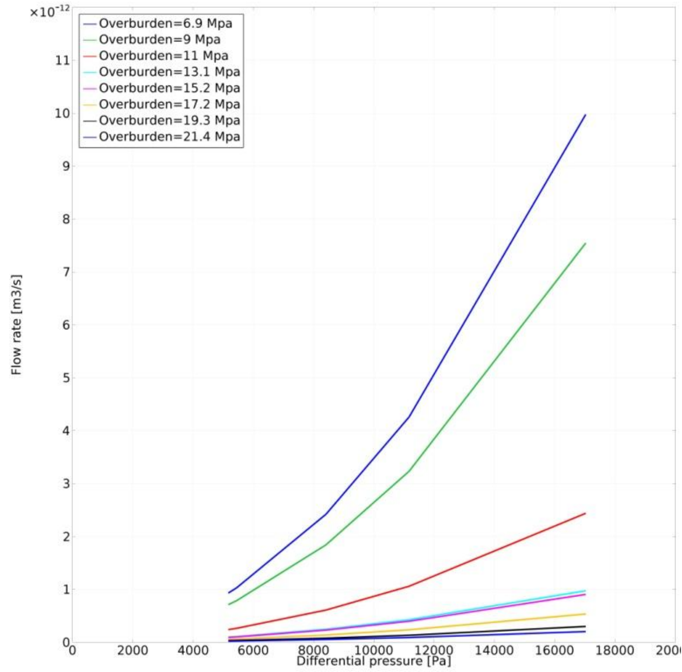

Fig. 7. Cross flow between matrix and fracture variation in response to the overburden stress when poro-elasticity and stress dependent permeabilities was not considered.

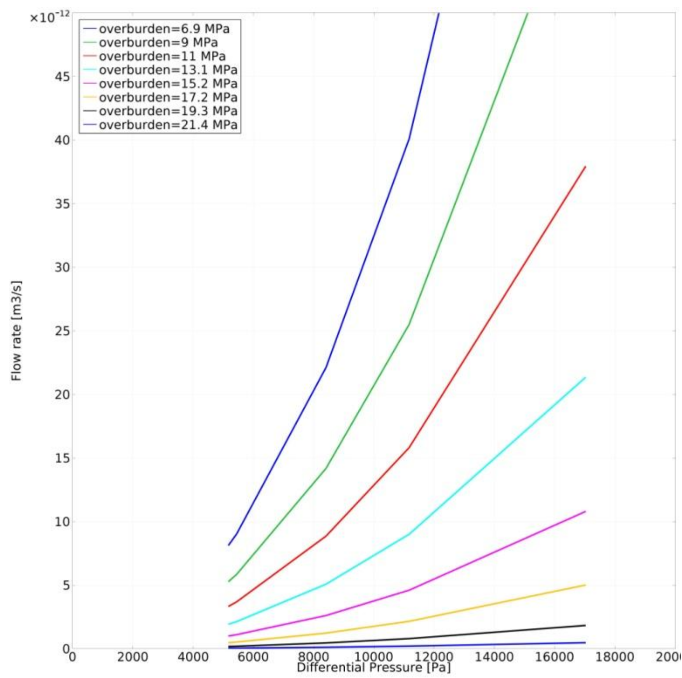

Fig. 8. Cross flow between matrix and fracture variation in response to the overburden stress when poro-elasticity and stress dependent permeability were taken into consideration.

Cross flow monitoring in both approaches reveals that primarily the flow discharge from matrix to the fracture decreases as the overburden stress increases. In fact at some excessive overburden stress, this flow exchange ceases and both systems flow individually. Being aware of the stress threshold beyond which matrix and fracture behave hydraulically independent will assist the engineers to formulate and implement appropriate stress relief strategy especially in highly-stressed fractured reservoir rocks to facilitate fracture networks hydrocarbon charging. This critical overburden stress is about 1.5e7 Pa for equivalent porous media approach (Fig. 7), whilst for the poro-elasticity coupled simulation it is 2.14e7 Pa (Fig. 8). This difference is an indication of the necessity of flow partitioning experimental data in which separate matrix and fracture flow rates are presented.

The other interesting finding is the significant difference between the calculated cross flow rates for the poro-elasticity coupled analysis in comparison with the equivalent porous medium analysis. The higher amount of cross flow together with previously discussed larger fracture apertures is responsible for the higher fracture flow partitioning in the poro-elasticity coupled study (Fig. 9).

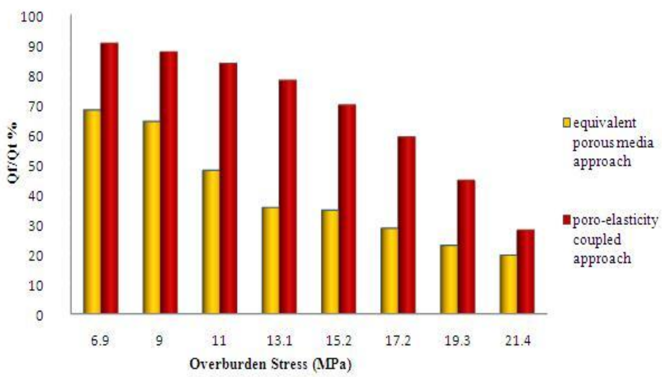

Fig. 9. Comparison of fracture flow partitioning between the equivalent porous medium and the poro-elasticity coupled modeling (Q_f and Q_t represent the outflow from fracture and the whole core respectively).

It is worth mentioning that a similar work using the same experimental data had considered the fracture as a 2D boundary within the geometry and used a tangential form of Darcy equation to calculate the flow rate within the fracture [16]; however by validation against cumulative outflow experimental data, the results were not even as accurate as those obtained from the equivalent porous medium approach used in this work. Therefore the poro-elasticity coupled model provides the most reliable outflow rate and fracture-matrix flow partitioning results.

7. CONCLUDING REMARKS

Three different flow equations were coupled in order to obtain the most reliable simulation of flow partitioning within a fractured porous media. These flow equations were further coupled with overburden stress effects in two different approaches – the equivalent porous medium and poro-elasticity coupled modeling. The poro-elasticity coupled analysis proved to be the most reliable approach in terms of the accuracy of the cumulative outflow results. It was shown that the equivalent porous medium simulation approach, can be misleading in flow partitioning investigations in terms of fracture flow, matrix flow and cross flow between the two hydraulic systems.

Cross flow evolution monitoring under various stress loading indicated a fracture healing pressure beyond which flow exchange between fracture and matrix reduces significantly and the charging of the fractures from the matrix, containing reservoir fluid, ceases. Having a proper understanding of this pressure would be useful in the prediction of fractured reservoir production under different stress regimes like during depletion of the reservoir over its lifecycle.

ACKNOWLEDGEMENT

The authors gratefully acknowledge the IDEAS Research Institute at Robert Gordon University for funding the research work on which this paper is based. The financial support from Aberdeen Formation Evaluation Society (AFES) to the first author to enable the presentation of this paper is also gratefully acknowledged.

REFERENCES

1. Kazemi, H., J.R. Gillman, and A.M. Elsharkawy. 1992. Analytical and numerical solution of oil recovery from fractured reservoirs with empirical transfer functions. Society of Petroleum Engineers Reservoir Engineering. May 1992: 219-227.

2. Pruess, K. and Y.S. Wu. 1991. A new semi-analytical method for numerical simulation of fluid and heat flow in fractured reservoirs. Society of Petroleum Engineers Advanced Technology Series. 1: 63-72

3. Akin, S. and A.R. Kovscek. 1999. Imbibition studies of low permeability porous media. In *Proceedings of SPE Western regional Meeting, Anchorage, 26 – 27 May 1999*.

4. Taniguchi, T. and E. Fillion. 1996. Numerical experiments for 3-dimensional flow analysis in a fractured rock with porous matrix. Advances in Water Resources. 19: 97-107.

5. Matthai, S.K., A. Mezentsev, and M. Belayneh. 2007. Finite element-node-centered finite-volume two-phase flow experiments with fractured rock represented by unstructured hybrid-element meshes. Society of Petroleum Engineers evaluation and Engineering. December 2007: 740-756.

6. Piri, M. and Z.T. Karpyn. 2007. Prediction of fluid occupancy in fractures using network modeling and X-ray micro tomography. Physical Review E. 76: No.016316.

7. Petchsingto, T. and Z.T. Karpyn. 2009. Deterministic modeling of fluid flow through a CT-scanned fracture using computational fluid dynamics. Energy Sources, Part A. 31: 897-905.

8. Petchsingto, T. and Z.T. Karpyn. 2010. Simulation of fluid percolation in a rough-walled rock fracture. Hydrogeology Journal. 18: 1,583-1,589.

9. Bai, M. and D. Elsworth. 1994. Modeling of subsidence and stress-dependent hydraulic conductivity for intact and fractured porous media. Rock Mechanics and Rock Engineering. 27, 4: 209-234.

10. Bai, M., F. Meng, D. Elsworth, M. Zaman, and J.C. Rogiers. 1997. Numerical modeling of stress-dependent permeability. Int. J. Rock Mech & Min. Sci. 34: 3-4. Paper No. 020.

11. Bai, M., F. Meng, D. Elsworth, and J.C. Rogiers. 1999. Analysis of stress-dependent permeability in nonorthogonal flow and deformation fields. Rock Mechanics and Rock Engineering. 32, 3: 195-219.

12. Crandall, D., G. Ahmadi, and D.H. Smith. 2010. Computational modeling of fluid flow through a fracture in permeable rock. Transp. Porous Med. 84: 493-510.

13. Stalker, R., G.M. Graham, and G. Oluyemi. 2009. Modeling stage diversion treatments and chemical placement in the presence of near-wellbore fractures. In *Proceedings of SPE oilfield Chemistry Symposium, Houston, 20 – 22 April 2009*.

14. Martys, N.S. and J.G. Hagedom. 2002. Multi scale modeling of fluid transport in heterogeneous material using discrete Boltzmann methods. Materials and structures. 35: 650-659.

15. Biot, M.A. 1962. Mechanics of deformation and acoustic propagation in porous media. J. Appl. Phys. 33: 1,482-1,498.

16. Sanaee, R., G.F. Oluyemi, M. Hossain, and M.B. Oyeneyin. 2012. Fracture-matrix flow partitioning and cross flow: numerical modeling of laboratory fractured core flood. In *Proceedings of the 2012 COMSOL conference, Milan, 10 – 12 October 2012*.